

Coronary Angiography

## Calculation of a Subject-Specific Adaptive Motion-Correction Factor for Improved Real-Time Navigator Echo-Gated Magnetic Resonance Coronary Angiography

Andrew M. Taylor, Jennifer Keegan, Permi Jhooti, David N. Firmin, and Dudley J. Pennell

Cardiovascular Magnetic Resonance Unit, Royal Brompton Hospital, Sydney Street, London, UK

### ABSTRACT

*There has been conflicting data in the literature regarding the use of wide navigator echo (NE) acceptance windows in combination with adaptive motion correction for magnetic resonance coronary angiography (MRCA). This in part may be due to the use of a fixed correction factor when applying the adaptive motion-correction algorithm, which may potentially result in miscorrection of the imaging slice in subjects whose correction factor differs widely from the mean. We have addressed this issue by measuring the superior/inferior correction factor in 25 subjects and assessing the effect of using a subject-specific correction factor ( $CF_{SS}$ ) for MRCA in comparison with no adaptive motion correction ( $CF_0$ ) and erroneous adaptive motion correction with a correction factor of 1.0 ( $CF_1$ ). There was a wide variation in the correction factor between subjects (proximal right coronary artery,  $0.49 \pm 0.15$ , range 0.20–0.70; proximal left coronary artery, mean  $0.59 \pm 0.15$ , range 0.20–0.85). The subject-specific correction factor was accurately calculated from motion of the aortic root in the coronal plane between expiratory and inspiratory breathhold (correction factor calculated from coronal image versus correction factor calculated after localization of coronary arteries,  $r = 0.92$ ,  $p < 0.001$ ). MRCA image quality was improved using a subject-specific correction factor, for both a 6-mm NE acceptance window ( $CF_{SS}$  versus  $CF_0$ ,  $p = 0.008$ ;  $CF_{SS}$  versus  $CF_1$ ,  $p = 0.02$ ) and a 16-mm NE window ( $CF_{SS}$  versus  $CF_0$ ,  $p = 0.01$ ;  $CF_{SS}$  versus  $CF_1$ ,  $p = 0.007$ ). Furthermore, image quality was maintained between the two NE windows if the subjects-specific correction factor was used (6 versus 16 mm,  $p = 0.21$ ), with an improvement in scan efficiency (6 versus 16 mm,  $49 \pm 17\%$  versus  $81 \pm 22\%$  respectively,  $p < 0.001$ ). Thus, for adaptive motion correction to be implemented, a subject-specific correction factor should be used and calculated from simple coronal expiratory and inspiratory breathholds. For real-time NE-gated cardiac MR with adaptive motion correction, the NE window can be widened to reduce the acquisition period without loss of image quality.*

**KEY WORDS:** Adaptive motion correction; Magnetic resonance coronary angiography; Navigator echoes; Respiratory motion compensation.

Received July 10, 1998; Accepted September 10, 1998  
Address reprint requests to A. M. Taylor.

## INTRODUCTION

Real-time, navigator echo (NE), respiratory-gated magnetic resonance coronary angiography (MRCA) can produce images of equivalent quality to breathholding while enabling improvements in image resolution and signal to noise, with much reduced patient cooperation (1). However, the respiratory position drifts over time, removing parts of the respiratory trace from the narrow NE acceptance window, which in turn leads to an increase in the acquisition period and image blurring (2). One method for dealing with this problem is to widen the NE acceptance window in combination with the application of adaptive motion correction. Adaptive motion correction techniques have been developed to enable motion correction during the acquisition of image data (3,4). Thus, for images acquired in a transaxial plane, superior/inferior motion of the coronary artery can be predicted from NE-monitored diaphragm motion and the coronary imaging slice moved to maintain the coronary artery within the imaging slice, compensating for changes in respiratory position (Fig. 1). A good linear relationship has been demonstrated between the superior/inferior motion of the proximal coronary arteries and the diaphragm. This is not a 1:1 relationship, and a correction factor is required to translate superior/inferior diaphragm motion to coronary motion (5). Correction factors of  $0.57 \pm 0.26$  for the proximal right coronary artery (RCA) and  $0.70 \pm 0.18$  for the proximal left coronary artery (LCA) have been reported (5).

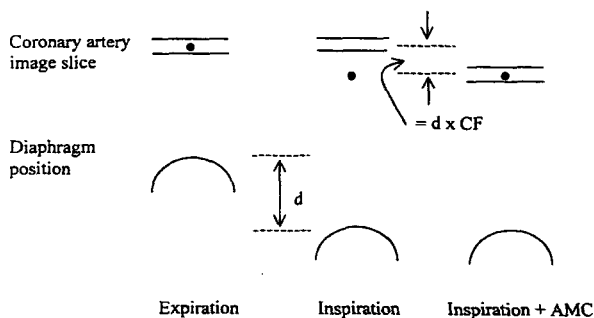


**Figure 1.** Schematic representation of adaptive motion correction (AMC). The coronary artery moves down during inspiration, out of the imaging plane. NE diaphragm monitoring measures this downward displacement ( $d$ ). From the linear relationship between superior/inferior diaphragm and coronary displacement, the superior/inferior coronary displacement can be predicted ( $d \times CF$ , where  $CF$  is the correction factor). Thus, the imaging slice select gradient is offset to include the coronary artery in the new imaging plane.

Adaptive motion correction has been used in combination with narrow NE acceptance windows (5–7 mm) to give improvements in image quality and slice registration (6). However, when wider NE acceptance windows (16–30 mm) have been used, the results have been conflicting. Wang et al. (7) demonstrated that image quality can be maintained and scan efficiency improved by using a wide NE acceptance window with adaptive motion correction, whereas Danias et al. (6) demonstrated poor image quality when using a wide NE acceptance window with adaptive motion correction. In both studies a fixed correction factor was used for all subjects imaged.

In this study, we demonstrate a wide variation in the superior/inferior correction factor between individuals. We describe a simple technique for calculating the subject-specific correction factor and demonstrate that MRCA image quality can be improved if this subject-specific correction factor is applied.

## METHODS

### Subjects and MR Imaging

Twenty-five subjects were studied supine (20 men and 5 women, mean age 45 years). MR imaging was performed with an “in-house” designed 0.5-T scanner using a rectangular surface coil ( $20 \times 15$  cm). An MR imaging console (Surrey Medical Imaging Systems, Surrey, UK) with additional hardware and software was used to generate and drive the gradient coils and radiofrequency waveforms and to receive and reconstruct the image data.

All images were acquired with a conventional two-dimensional MRCA sequence during mid to late diastole and the following parameters: TE 6.7 msec, TR 12 msec, slice thickness 5 mm, field of view  $30 \times 30$  cm, in-plane resolution  $1.2 \times 2.3$  mm, number of excitations 1, number of views per segment 8, incremental flip angle  $35\text{--}90^\circ$ . The NE pulse was performed 65 msec before image data acquisition, and a fat saturation pulse was applied immediately before image data acquisition. The study was approved by the Royal Brompton Hospital Ethical committee, and all subjects gave informed consent.

### Diaphragm Monitoring

Coronal and transverse pilot scans were performed to identify the dome of the right hemidiaphragm. The NE was defined by the intersection of orthogonal slice-selective  $90$  and  $180^\circ$  radiofrequency pulses. A correlation algorithm was implemented for diaphragm edge detection. The acquisition parameters for the NE pulse were as follows: pulse duration 4 msec, field of view along the col-

umn length 512 mm, readout points 512, data sampling time 10 msec, column area  $2 \times 2$  cm.

### Calculation of Individual Correction Factors

#### Two-Point Method

For all 25 subjects, a correction factor was calculated from expiratory and inspiratory breathholds during NE diaphragm monitoring. Expiratory and inspiratory diaphragm positions were derived from the NE traces and coronary positions measured directly from the acquired images. The correction factor was then calculated as the ratio of superior/inferior coronary to diaphragm motion. The inspiratory and expiratory breathholds were per-

formed for both a coronal pilot at the start of scanning (Fig. 2A) and after localization of the coronary arteries (Fig. 2B). For the coronal pilot, changes in the inferior border of the right-sided aortic sinus were used as to estimate proximal RCA motion and the superior border of the left aortic sinus for LCA motion.

#### Seven-Point Method

For 10 subjects, the LCA correction factor was calculated from seven breathhold images centered 5 mm apart (total range of diaphragm motion, 30 mm). Proximal LCA images were acquired in a sagittal plane just distal the left main stem origin. An NE feedback system was used to guide the subjects to their breathhold positions,

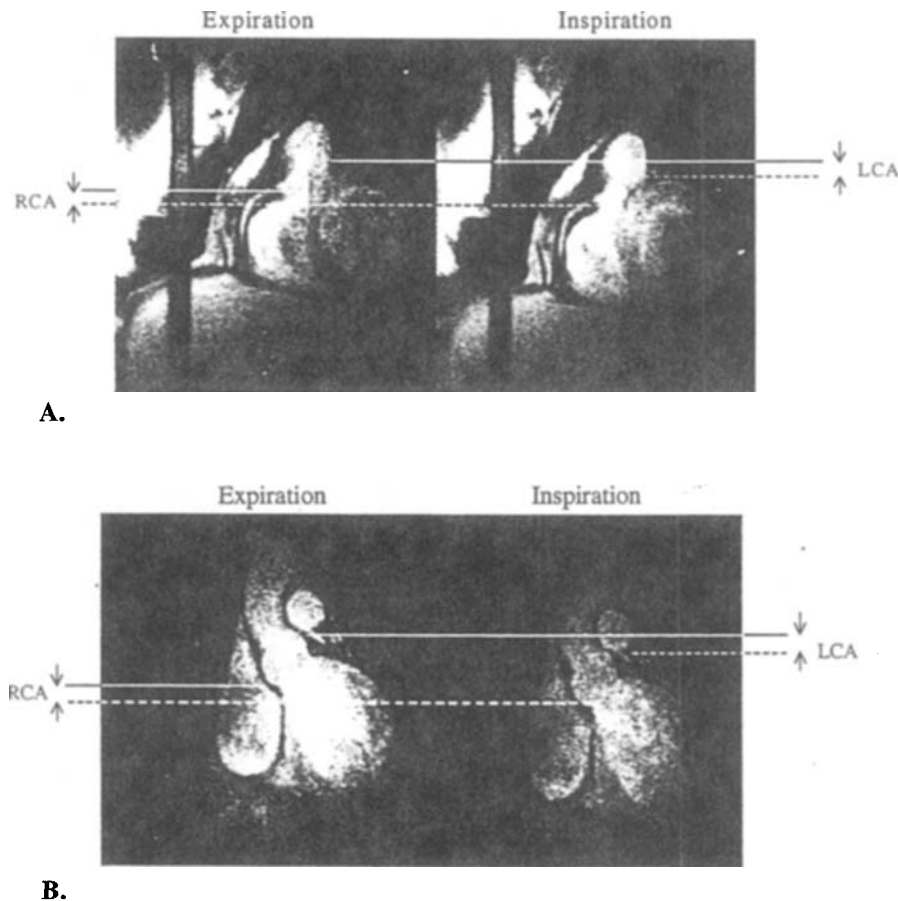


**Figure 2.** Calculation of the correction factor from expiratory and inspiratory breathholds. (A) For the coronal image, changes in the inferior border of the right aortic sinus were used to estimate RCA motion. For the estimate of LCA motion, changes in the superior border of the left aortic sinus were used. (B) For the coronary images, changes in the inferior surface of the in-plane RCA origin and in the inferior surface of the through-plane LCA were used to measure coronary motion. For all images, changes in the diaphragm position between the two breathholds were measured from the NE traces.

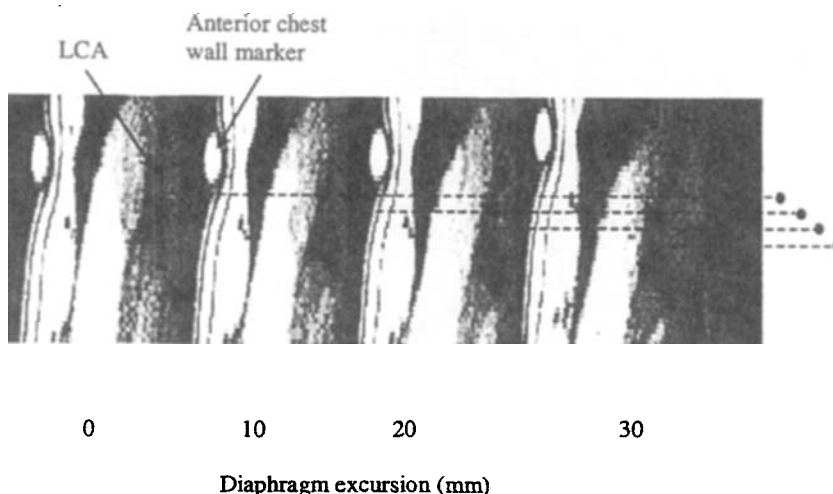


**Figure 3.** Sagittal images of the LCA through-plane are shown at four different breathhold positions 10 mm apart. Changes in the LCA position were measured directly from the images. Diaphragm position was measured from the NE traces.

with a narrow NE acceptance window of 2 mm to ensure consistent breathholding. Again, the NE traces yielded information about superior/inferior changes in diaphragm motion, and superior/inferior coronary motion was measured directly from the images (Fig. 3). The correction factor was calculated from a plot of diaphragm displacement against coronary displacement (gradient of linear regression line).

#### Adaptive Motion-Correction MRCA

For the remaining 15 subjects, transaxial images of the RCA origin were acquired during free respiration using real-time NE gating with adaptive motion correction. The adaptive motion-correction algorithm calculates the difference between the recorded NE diaphragm position and the center of the NE acceptance window. The image slice select gradient is then offset, in real-time, by the product of this difference and the correction factor. The NE acceptance window was set at both 6 and 16 mm, and three correction factors were used: the subject-specific correction factor ( $CF_{SS}$ ), an erroneous correction factor of 1.0 ( $CF_1$ ), and no adaptive motion correction ( $CF_0$ ). Thus, six images were acquired for each subject. Image quality was scored by two independent blinded observers as follows: 1, unable to visualize coronary artery; 2, coronary artery visualize but severe blurring present; 3, coronary artery visualize but some blurring present; 4, coronary artery visualize and no blurring. Where image scores differed between observers, a consensus score was given.

For all MRCA images, scan efficiency (ratio of NEs accepted to NEs performed) was calculated.

#### Statistical Analysis

Linear regression was used to compare the estimate and actual correction factors and the two-point and seven-point methods for calculating the correction factor. The Wilcoxon signed rank test was used to compare differences in the image scores between the adaptive motion correction techniques. The paired Student's *t*-test was used to compare the scan efficiency data. A  $p < 0.05$  was regarded as significant. The statistical package SPSS for Windows (SPSS Inc., Chicago, IL) was used for the statistical analysis.

## RESULTS

For all subjects, the two-point subject-specific correction measured from the direct image of each coronary artery in-plane were RCA  $0.49 \pm 0.15$  and LCA  $0.59 \pm 0.15$ . There was a wide range of the correction factors for all individuals (0.20–0.85) (Fig. 4A).

There was a good correlation between the subject-specific correction factor calculated from the coronal pilot and the subject-specific correction factor calculated from the in-plane coronary images for both the RCA ( $r = 0.92$ ,  $p < 0.001$ ) and the LCA ( $r = 0.92$ ,  $p < 0.001$ ) (Fig. 4B).

The seven-point calculation method demonstrated a good linear relationship between superior/inferior mo-

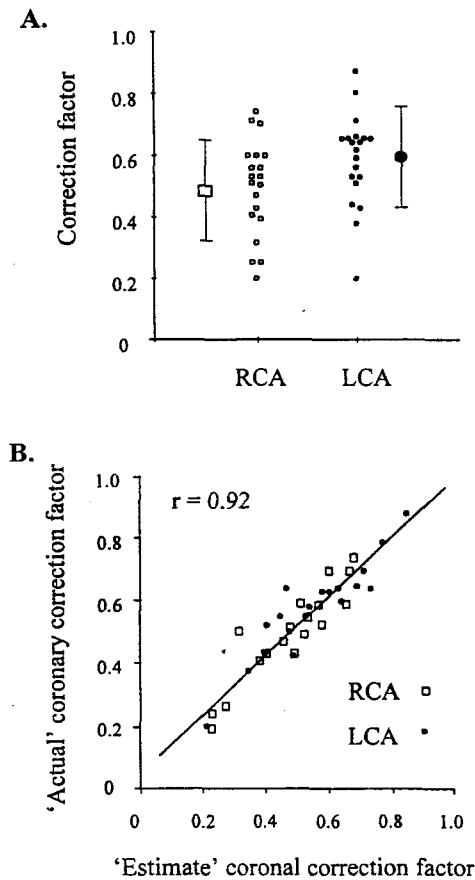


**Figure 4.** (A) Graphic representation of the two-point subject-specific correction factors measured from the direct coronary images for RCA and LCA. Mean values  $\pm$  SD are also shown, but note wide variation in calculated correction factors. (B) Plot of estimate correction factor, measured from the coronal images, against actual correction factor, measured after localization of the coronary arteries. The linear regression line for both RCA and LCA values is shown.

tion of the diaphragm and superior/inferior motion of the proximal LCA for each of the 10 subjects (mean correlation coefficient for all 10 subjects,  $r = 0.97 \pm 0.07$ ) (Fig. 5A). There was also good agreement between the coronary two-point and seven-point methods for calculating the subject-specific correction factor ( $r = 0.86$ ,  $p = 0.001$ ) (Fig. 5B).

For the RCA origin images, there was a significant improvement in image quality for the 6-mm NE acceptance window if the subject-specific correction factor was used compared with no adaptive motion correction ( $p = 0.008$ ) or erroneous adaptive motion correction ( $p =$

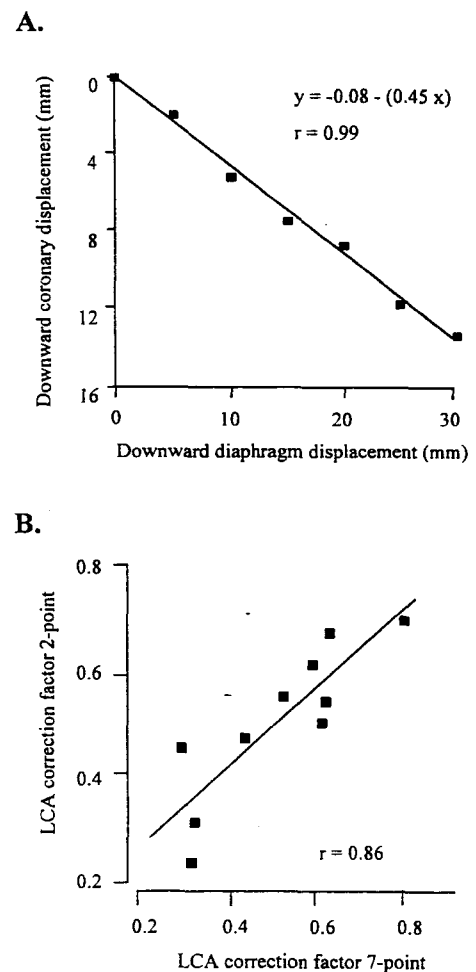


**Figure 5.** (A) Plot of superior/inferior diaphragm displacement against superior/inferior coronary displacement for a single subject. Linear regression line is shown. The gradient of this line is the subject's seven-point correction factor. (B) Plot of LCA correction factor calculated with the two-point method against the seven-point method. The linear regression line is shown.

0.02) (Fig. 6). Similarly, for the 16-mm NE window, images were significantly improved if the subject-specific correction factor was used ( $CF_{SS}$  versus  $CF_0$ ,  $p = 0.01$ ;  $CF_{SS}$  versus  $CF_1$ ,  $p = 0.007$ ) (Fig. 6). Furthermore, image quality was maintained between the two NE windows if the subject-specific correction factor was used (6- versus 16-mm NE window,  $p = 0.2$ ) (Fig. 7). Finally, there was a significant improvement in the scan efficiency when the wider NE window was used (6 versus 16 mm,  $49 \pm 17\%$  versus  $81 \pm 22\%$  respectively,  $p < 0.001$ ).

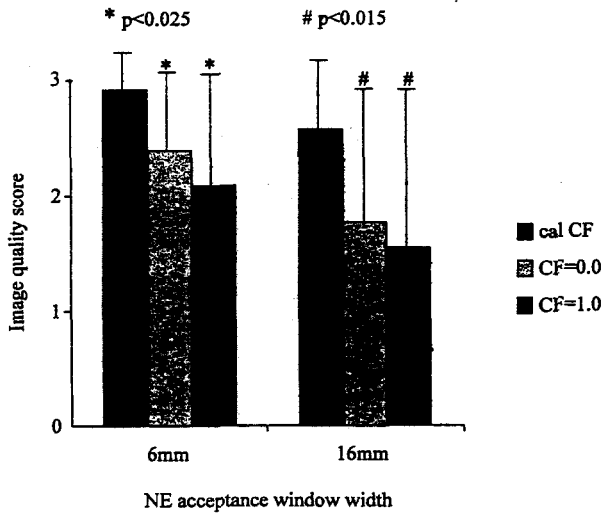


**Figure 6.** Averaged RCA origin image scores for all 15 subjects. High scores represent good image quality, and error bars represent SD. For the 6-mm NE acceptance window, image quality was significantly better when the subject-specific correction factor was used ( $*p < 0.025$ ). For the 16-mm NE window, image quality was also significantly improved when the subject-specific correction factor was used ( $\#p < 0.015$ ).

**DISCUSSION**

Motion of the coronary arteries is complex, with translational (superior/inferior, left/right, anterior/posterior), rotational, and deformational components. In this study, we concentrated on correcting for the respiratory motion in the superior/inferior direction when performing MRCA.

We demonstrated that a wide variation in the correction factor exists between individual subjects. However, a subject-specific correction factor can be accurately calculated at the start of MRCA imaging by acquiring coronal images of the aortic root during expiratory and inspiratory breathholds. Changes between the two breathholds can be calculated for both the diaphragm position (from the NE diaphragm traces) and the proximal coronary arteries (directly from the images using the inferior border of the right aortic sinus for the RCA and superior border of the left aortic sinus for the LCA). For all subjects, the mean correction factor for both the RCA and LCA calculated from this study was less than those seen by Wang et al. (5) (RCA, 0.49 versus 0.57, and LCA, 0.59 versus 0.70). This reflects differences in the portion of the diaphragm monitored between the two studies. In the study by Wang et al., diaphragm position was measured

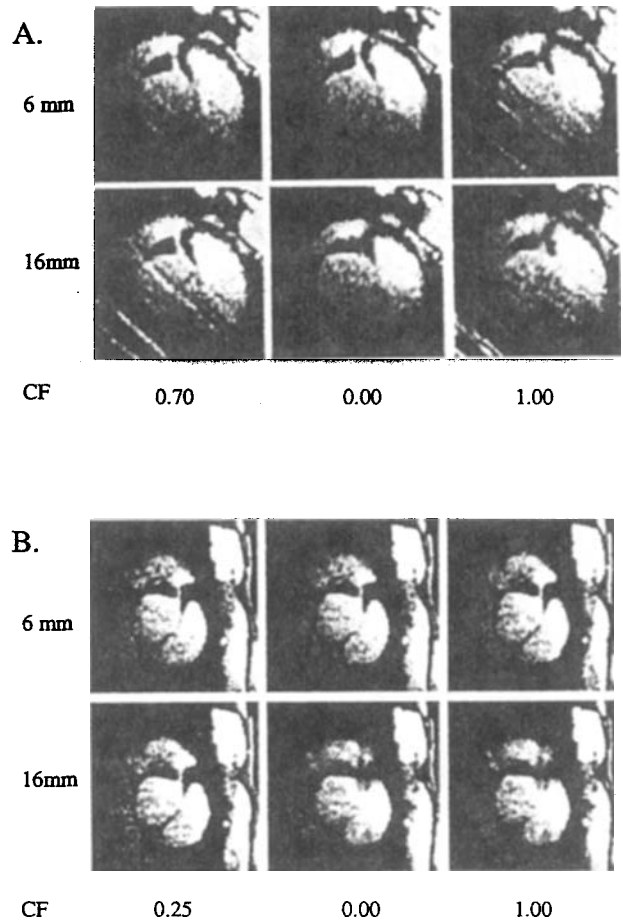


**Figure 7.** RCA origin images for two subjects are shown. (A) Individual correction factor, 0.70. For the 6-mm NE acceptance window, image quality is poor if erroneous correction is implemented (correction factor, 1.00). For the 16-mm NE window, image quality is only maintained when the subject-specific correction factor is used. (B) Individual correction factor, 0.25. For the 6-mm NE acceptance window, image quality is good for all correction factors used. Image quality is again only maintained for the 16-mm NE window when the subject-specific correction factor is used.

directly from the images at the inferior margin of the left ventricle, whereas motion of the dome of the right hemidiaphragm was assessed in the current study.

Implementation of real-time NE-gated MRCA, with adaptive motion correction and a subject-specific correction factor, improved image quality when compared with images acquired using no adaptive motion correction (i.e., NE gating alone) or an erroneous correction factor for both narrow (6 mm) and wide (16 mm) NE acceptance windows. There have been conflicting results with

the use of adaptive motion-correction and wide NE-acceptance windows (6,7). However, in the previous studies, a fixed correction factor has been used for all subjects. Thus, for some subjects the fixed correction factor may have been erroneous, leading to slice miscorrection and reduced image quality. The major advantages of using a wider NE window are that the imaging time can be reduced (improved scan efficiency) and drifting of the diaphragm end-expiratory position out of the NE window is limited.

Recently, it has been suggested that NE monitoring of the left ventricle may be easier to perform than NE diaphragm monitoring (8). One advantage of direct left ventricular motion gating is that superior/inferior motion of the coronary artery is being monitored. Thus, if adaptive motion correction is used, a subject-specific correction factor is not required because a 1:1 relationship exists between the NE-monitored position and the coronary position. However, for spin-echo NE monitoring, an NE image artifact can often be seen, and this may mimic signal loss secondary to a coronary stenosis. Furthermore, with the increasing use of intravascular contrast agents in combination with myocardial tissue suppression (9), high pulmonary vessel signal intensity and reduced myocardial intensity may make it more difficult to find a stable navigator signal on the heart.

### Study Limitations

In our study, an erroneous correction factor of 1.0 was used to emphasize the problems of using an inappropriate correction factor for all subjects studied. For both the 6- and 16-mm NE acceptance windows, there was a trend toward better image quality when no adaptive motion correction was used instead of adaptive motion correction with an erroneous correction factor, suggesting that image quality is reduced when miscorrection is performed. It could be argued that to make a true comparison to the previous work, the fixed correction factor of 0.6 should have been used. This would have required larger patient numbers, which was outside the scope of this study.

Two main limitations of using a wide NE acceptance window must be considered. First, because image data are accepted during all portions of the respiratory cycle, some data will be acquired during periods of high respiratory motion, leading to image blurring. In our study, there was a slight reduction in image quality when the wider window was used for all correction factors, and this may reflect the inclusion of data acquired during periods of rapid diaphragm motion. However, this effect of diaphragm motion during the read-out period can be reduced

by the use of fast imaging sequences (Spiral versus FLASH, read-out 20 versus 108 msec, respectively). Second, other components of coronary motion (e.g., anterior/posterior, left/right motion), which are not large when a narrow NE window is used, may become significant with wider NE windows. The effects of these components of motion need to be addressed, and it may be necessary in the future to use multiple NEs to monitor motion in several directions and compensate for overall motion of the coronary arteries.

### CONCLUSIONS

If adaptive motion correction is to be used in combination with real-time NE-gated cardiac MR, a subject-specific correction factor should be calculated at the start of the scan period. This subject-specific correction factor can be simply and accurately calculated by measuring changes in the superior/inferior position of the aortic root in a coronal plane between an expiratory and inspiratory breathhold. If a reduction in the scan acquisition period and/or compensation for diaphragmatic drift are also required, the NE acceptance window can be widened and image quality maintained when adaptive motion correction and a subject-specific correction factor are implemented. With wide NE windows, the read-out period of the imaging sequence should be as short as possible to reduce the effects of diaphragm motion during data acquisition.

### ACKNOWLEDGMENTS

Supported by the Coronary Disease Research Association (to A.M.T., J.K., P.J., D.N.F.).

### REFERENCES

1. Oshinski JN, Hofland L, Mukundan S, Dixon WT, Parks WJ and Pettigrew RI. Two-dimensional coronary MR angiography without breathholding. *Radiology*, 1996; 201: 737-743.
2. Taylor AM, Jhooti P, Wiesmann F, Keegan J, Firmin DN and Pennell DJ. Magnetic resonance navigator-echo monitoring of temporal changes in diaphragm position: Implications for magnetic resonance coronary angiography. *J Magn Reson Imag*, 1997; 7:629-636.
3. Ehman RL and Felmlee. Adaptive technique for high-definition MR imaging of moving structures. *Radiology*, 1989; 173:255-263.
4. Felmlee JP, Ehman RL, Riederer SJ and Korin HW. Adap-

- tive motion compensation in MRI: accuracy of motion measurement. *Magn Reson Med*, 1991; 18:207–213.
5. Wang Y, Riederer SJ and Ehman RL. Respiratory motion of the heart: Kinematics and the implications for spatial resolution in coronary imaging. *Magn Reson Med* 1995; 33:713–719.
  6. Danias PG, McConnell MV, Khasgiwala VC, Chuang ML, Edelman RR and Manning WJ. Prospective navigator correction of image position for coronary MR angiography. *Radiology*, 1997; 203:733–736.
  7. Wang Y, Johnston DL, Riederer SJ and Ehman RL. Adaptive motion correction for real-time Navigator gated coronary MR angiography. In: *Proceedings of the 4th annual meeting of the International Society for Magnetic Resonance in Medicine*. New York: International Society for Magnetic Resonance in Medicine; 1996:175.
  8. McConnell MV, Khasgiwala VC, Savord BJ, Chen MH, Chuang ML, Edelman RR and Manning WJ. Comparison of respiratory suppression methods and navigator locations for MR coronary angiography. *AJR Am J Roentgenol*, 1997; 168:1369–1375.
  9. Taylor AM, Panting JR, Keegan J, Gatehouse PD, Jhooti P, Yang GZ, Francis JM, Burman ED, McGill S, Firmin DN and Pennell DJ. Gradient echo cine and spin echo imaging of the heart, using the intravascular contrast agent, NC100150 injection. *JCMR*, 1999; 1:23–32.